

11th International Conference on Technology of Plasticity, ICTP 2014, 19-24 October 2014,  
Nagoya Congress Center, Nagoya, Japan

## Analytical and FEM investigations on boss forming process by compression–drawing method

Wenzheng Dong<sup>a</sup>, Qiquan Lin<sup>a,\*</sup>, Yantao Li<sup>a</sup>, Zhigang Wang<sup>b</sup>

<sup>a</sup>*School of Mechanical Engineering, Xiangtan University, Hunan, Xiangtan, 411105, China*

<sup>b</sup>*Department of Mechanical and Systems Engineering, Gifu University, Yanagido, Gifu, 501-1193, Japan*

---

### Abstract

In plate forging process, one of the major causes for dimple defect is large processing load with the nonuniform material flows of local plastic deformation. In the present work, a new solid boss forming process named compression-drawing method was proposed with a lower forming load. The theoretical formula of the radii of separation flow was deduced based on slab method, in which the radii of separation flow decreases gradually as the bottom thickness decreases. The finite element method (FEM) with DEFORM-3D was used to investigate the solid boss forming process. The results show that the boss height is found insufficient when the punch pressure is under 200KN while the fracture behavior occurs as the punch pressure reaches 670KN approximately. The FEM calculations are well agreement with the experimental results.

© 2014 Published by Elsevier Ltd. This is an open access article under the CC BY-NC-ND license (<http://creativecommons.org/licenses/by-nc-nd/3.0/>).

Selection and peer-review under responsibility of the Department of Materials Science and Engineering, Nagoya University

**Keywords:** Solid boss forming; Compression–drawing method; Dimple defect; DEFORM-3D; Slab method

---

### 1. Introduction

Considering the advantages of miniaturization, light weight and low cost, solid boss structures are widely used to simplify the components in manufacturing industry. Traditionally, the backward extrusion process is adopted to

---

\* Corresponding author. Tel.: +86-731-58292209; fax: +86-731-58292210.  
E-mail address: [xtulqq@163.com](mailto:xtulqq@163.com)

form the solid boss structures, which would bring several unsatisfactory limitations, such as the large processing load, the less boss height and especially the serious dimple defect occurred in the bottom part.

To improve the formability of sheet metal, the bulk forming processes are applied to sheet metal forming processes, generally referred to as sheet-bulk metal forming processes (Merklein et al., 2012). For one thing, lots of sheet-bulk metal forming processes are developed to form the complex functional components recently, such as deep-drawing upsetting process (Schneider et al., 2011), hole-flanging extrusion process (Lin et al., 2007), upsetting burring process (Dohda et al., 2004), plate forging process of tailored blanks having local thickening for deep drawing of square cups (Mori et al., 2011). For another, pressing forging processes has been applied to light alloy sheets (Sheng et al., 2006, Chen, et al., 2007).

In our previous work, a novel sheet-bulk metal forming process named compression-drawing were proposed to form the solid boss on a plate product with a lower forming load (Lin, et al., 2010, Wang et al., 2012, Wang et al., 2013). In this paper, the theoretical formula of separation flow radii  $R$  and punch pressure were deduced based the on slab method. The finite element method (FEM) with DEFORM-3D was used to investigate the solid boss forming process. Besides, the boss forming limit and the evolution of dimple defect that occurred in solid boss forming process were investigated.

## 2. FEM simulation and experimental conditions

Fig. 1 shows the geometric model and FEM model of the compression-drawing process. Due to symmetry, only one-sixth of the part was used for the FEM simulation model to reduce the calculated time, as seen in Fig. 1(b). In this study, a commercial analytical code for statistic implicit finite element method (DEFORM-3D) was used as the FEM simulation tool. Table 1 shows the details of the FEM simulation conditions and the tool dimensions. The workpiece material was set as a rigid-plastic type with aluminum A1050-O (JIS). The constitutive equation was determined from the stress-strain curve obtained by the tensile testing experiment, as shown in Table 1, specifically the strength coefficient and strain hardening exponent values were 168MPa and 0.12, respectively.

Besides, with the same FEM simulation conditions, the laboratory experiments were carried out on an 1100kN servo press KOMATSU H1F110 to validate the FEM simulation results. The punch load was measured with a load cell installed in the press and the paraffinic mineral oil P460 was applied for lubrication.

## 3. Theoretical derivation of radii of separation flow surface

To examine the boss forming limit in compression-drawing, a separation flow surface was discovered during the solid boss forming process, as shown in Fig. 2(a). Since the bottom part of blank is the main deformation zone in solid boss forming process, four different zones are divided to calculate the radii of separation flow surface, as shown in Fig. 2(a).

Based on the slab method, the stress distributions of four plastic zones are characterized in Fig. 2(b). As shown in Zone 1, the equilibrium equation and simplified yield criterion for boss part can be written as

$$\sigma_z \pi r^2 - (\sigma_z + d\sigma_z) \pi r^2 - 2\pi r \tau dz = 0, \quad (1)$$

$$\sigma_r - \sigma_z = 2K, \quad (2)$$

where  $\sigma_z$  is the radial stress, and  $\sigma_r$  is the circumferential stress,  $\tau$  is shear stress,  $K$  is the shear yield stress of blank. Based on the constant friction conditions,  $\tau$  can be expressed by

$$\tau = mK, \quad (3)$$

where  $m$  is the friction factor in Zone 1. Substitution of the boundary condition  $z = 0$  into Eq. (3),  $p$  can be expressed by

$$p = \sigma_z|_{z=0} = 2\tau h / r = 2mKh / r. \quad (4)$$

Similarly, for Zone 2, the simplified yield criterion is:

$$p_1 - p = 2K. \quad (5)$$

According to the statical equilibrium along the horizontal direction, the equilibrium equations for Zone 3 and Zone 4 can be written as

$$p_1 2\pi(r+r_b)t + \tau' \pi [R^2 - (r+r_b)^2] + \tau'' \pi [R^2 - (r+r_b)^2] = p_2 2\pi R t, \quad (6)$$

$$p_3 2\pi R t + \sigma_p 2\pi(r_1 - r_p)t = \tau' \pi [(r_1 - r_p)^2 - R^2] + \tau'' \pi [(r_1 - r_p)^2 - R^2], \quad (7)$$

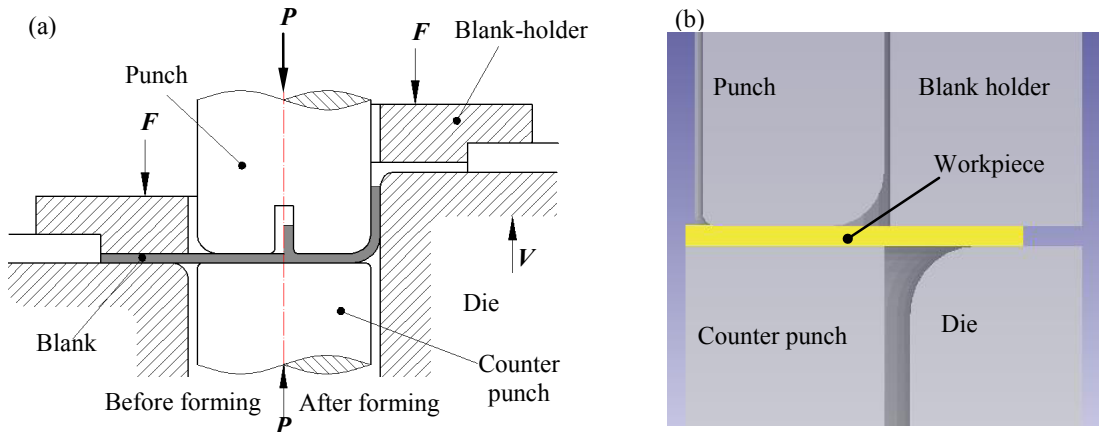


Fig. 1. (a) Geometric model and (b) FEM model of compression-drawing process.

Table 1. FEM simulation conditions.

Name	Analysis condition
Number of elements	40000
Workpiece	Diameter: 60(mm)/ Thickness: 2(mm) Object type: Rigid-Plastic A1050-O(JIS),Material flow curve: $\sigma = 168(\varepsilon + 0.02)^{0.12}$
Punch	Diameter: 40(mm)/ Profile radius: 4.5(mm)
Die	Boss diameter: 2.5( mm)/ Boss profile radius: 1(mm)
Counter punch	Inner diameter: 45.2(mm)/ Profile radius:4.5(mm) Diameter: 40(mm)

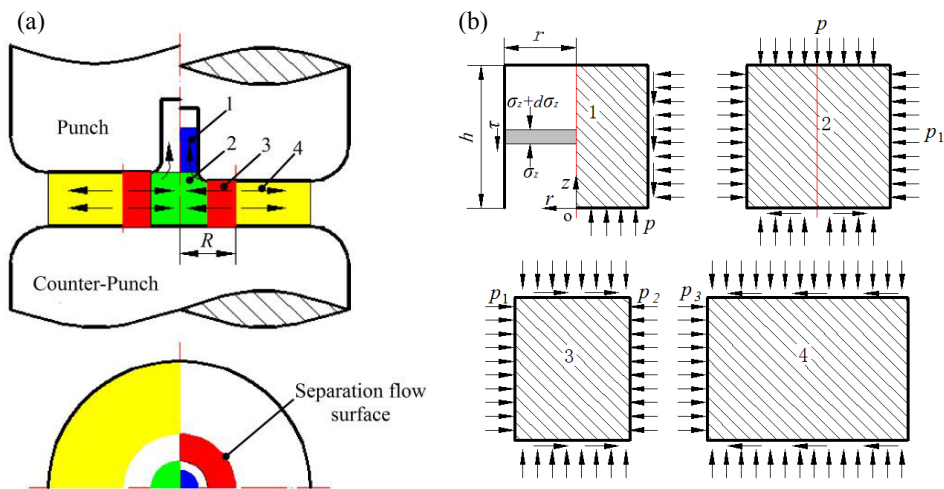


Fig. 2. Four different deformation zones in bottom part (a) and stress distributions (b).

where  $p_2 = p_3$ ,  $\sigma_\rho$  is the radial stress induced by deep drawing,  $\tau' = m'K$ ,  $\tau'' = m''K$ ,  $m'$  and  $m''$  are the friction factor in the upper and lower surface of Zone 1. Accordingly, the radii of separation flow surface can be obtained by combining Eq. (4), Eq. (5), Eq. (6) and Eq. (7),

$$R = \frac{\sqrt{2}}{2} \sqrt{(r+r_b)^2 + (r_1-r_p)^2 - \frac{(2mK \frac{h}{r} + 2K)(r+r_b) + \sigma_\rho(r_1-r_p)}{(m' + m'')K} t}. \quad (8)$$

For Zone 3, the  $\sigma_{z3}$  can be obtained as

$$\sigma_{z3} = -\frac{\tau' + \tau''}{t} r_x + C', \quad (9)$$

where  $C'$  is a constant, and it can be obtained by the boundary condition:  $r_x = r+r_b, \sigma_{z3} = p$

$$C' = p + \frac{(\tau' + \tau'')(r+r_b)}{t}. \quad (10)$$

Substitution of Eq. (10) into Eq. (9), one can obtain

$$\sigma_{z3} = \frac{\tau' + \tau''}{t} (r+r_b - r_x) + p. \quad (11)$$

Thus, the stress at the separation flow surface can be calculated by Eq. (11) as

$$\sigma_{z3}|_{r_x=R} = \frac{\tau' + \tau''}{t} (r+r_b - R) + p. \quad (12)$$

Similarly, for zone 4, the  $\sigma_{z4}$  can be obtained as

$$\sigma_{z4}|_{r_x=R} = \frac{\tau' + \tau''}{t} (r_1 - r_p - R) + 2K - \sigma_p. \quad (13)$$

Combining Eq. (12), Eq. (13) and  $\sigma_{z3}|_{r_x=R} = \sigma_{z4}|_{r_x=R}$ , one can obtain

$$\sigma_p = 2K - p + \frac{\tau' + \tau''}{t} (r_1 - r_p - r - r_b) = 2K - p + \frac{(m' + m'')K}{t} (r_1 - r_p - r - r_b). \quad (14)$$

Combining Eq. (8) and Eq. (14), one can obtain

$$R = \sqrt{\frac{1}{2} (r+r_b)(r+r_b+r_1-r_p) - \left[ \left( \frac{m}{m' + m''} \frac{h}{r} + \frac{1}{m' + m''} \right) (r+r_b) + \left( \frac{1}{m' + m''} - \frac{m}{m' + m''} \frac{h}{r} \right) (r_1-r_p) \right] t}. \quad (15)$$

Thus, the theoretical calculation of punch pressure can be obtained as

$$P = \int_0^{r+r_b} p 2\pi r_x dr_x + \int_{r+r_b}^R \sigma_{z3} 2\pi r_x dr_x + \int_R^{r_1-r_p} \sigma_{z4} 2\pi r_x dr_x. \quad (16)$$

Substitution of Eq. (4), Eq. (12) and Eq. (13) into Eq. (16), the theoretical calculation of punch pressure can be written as

$$P = 2\pi K \left\{ \frac{2mh}{r} (r+r_b)^2 + \left[ \frac{(r+r_b)(m' + m'')}{2t} + \frac{mh}{r} \right] [(r_1-r_p)^2 - (r+r_b)^2] - \frac{m' + m''}{3t} [(r_1-r_p)^3 - (r+r_b)^3] \right\}. \quad (17)$$

From Eq. (17), we can easily estimate the punch pressure based on the given boss structure, die structure, frictional conditions and material properties.

## 4. Results and discussion

### 4.1. Boss forming limit

In the boss forming process by compression-drawing method, punch pressure plays an important role in controlling the boss forming ability. From Eq. (4) as discussed above, we can easily estimate the proper punch pressure based on the given boss structure, although other extrinsic factors are neglected, namely, the additional

drawing force in compression-drawing process. Thus, it is found than an over or under estimation occurs compared with the experimental results, as shown in Fig. 3(a). From Fig. 3(a), the boss height increases as the punch pressure increases, and the FEM calculations are well agreement with our experimental results. When the punch pressure is under 200 kN, the boss height is insufficient since the pressures are too small to push the materials to the boss cavity. However, the undesired fracture behavior is expected to occur at the punch shoulder as the punch pressure reaches about 670 kN, as shown in Fig. 4. According to our FEM analysis, it is found that fracture behavior occurs when the radial stress reaches about 110 MPa, which is almost the same as the tensile strength of A1050-O, 115 MPa, as shown in Fig. 3(b).

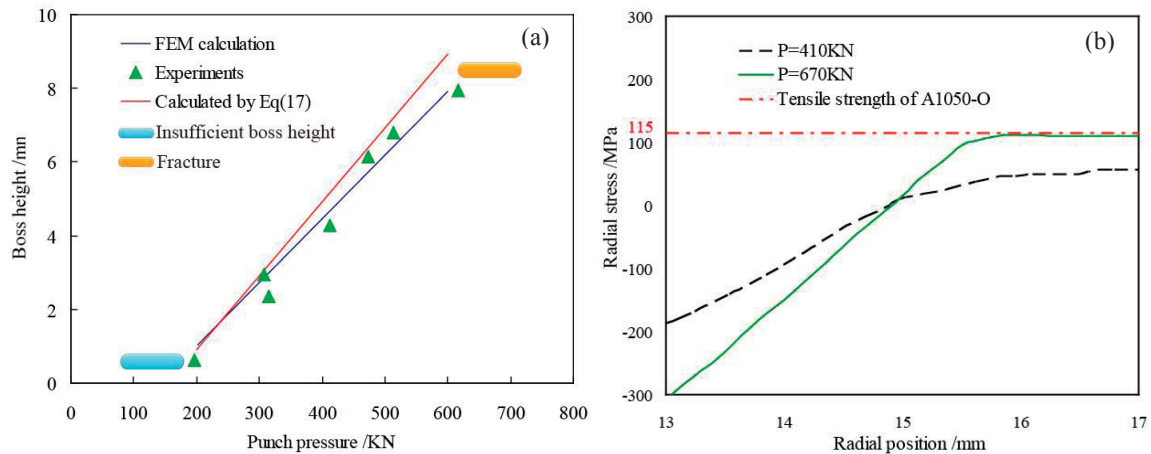


Fig. 3. (a) Boss forming limit in compression-drawing process and (b) FEM analysis of radial stress distribution along radial direction.



Fig. 4. Product samples by compression-drawing process with A1050-O sheet under different punch pressures ((a) 410kN, (b) 670kN).

#### 4.2. Separation flow surface

In our FEM simulations, the characteristic of separation flow surface can be illustrated by the material velocity. From Eq. (15) discussed above, the theoretical radii of separation flow surface is effected by the die structure and the friction conditions.

The relationship between the radii of separation flow surface and bottom thickness is shown in Fig. 5. Since the upper surface of blank is only lubricated in the experiments, the friction factors in upper and lower surface of blank are 0.3 and 0.8 respectively. Obviously, the radii of separation flow surface decreases gradually as the blank thickness decreases. When the blank thickness reaches the minimum value, the radii of separation flow surface stays a stable value until the boss forming process is over. There is reasonable concordance between the theoretical calculation and FEM during the first half part of the process, as shown in Fig. 5. However, at the later stage, an underestimate value is predicted by FEM calculation, which may be caused by the mesh distortions in the sheet bottom part.

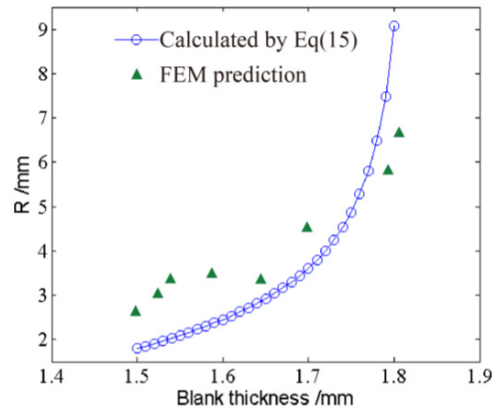


Fig.5. Relationship between the blank thickness and radii of separation flow surface ( $h=5.8\text{mm}$ ,  $m=0.5$ ,  $m'=0.3$ ,  $m''=0.8$ ,  $P=480\text{kN}$ ).

## 5. Conclusions

In this paper, based on the slab method of the boss forming part, we have established the theoretical relationship between the radii of separation flow and bottom thickness of sheet blank, and the radii of separation flow increases rapidly as the bottom thickness decreases. The boss forming limit and dimple defect are investigated by FEM analysis, which are well agreement with our experimental results.

## Acknowledgements

This work is supported by the National Natural Science Foundation of China (No. 51175445) and Hunan Provincial Innovation Foundation for Postgraduate (No. CX2013B277).

## References

- Chen, F.K., Huang, T.B., Wang, S.J., 2007. A study of flow-through phenomenon in the press forging of magnesium alloy sheets, *Journal of Materials Processing Technology*, 188-187, 770-774.
- Dohda, K., Wang, Z.G., Yokoyama, N., Kobayashi Y., Hirasawa, K., 2004. Development of new burring process for thick plates. *Transactions of NAMRI/SME*, 32, 183-190.
- Hurakami, H., Saaski, B., Yoneoka, S., Ohtake, N., Yasuhara, T., 2007. Method for preventing dimple defects on light sheet metal in boss forming. *Journal of the JSTP*, 48(555), 293-297. (in Japanese).
- Lin, H.S., Tung, C.W., 2007. An investigation of cold extruding hollow flanged parts from sheet metals. *International Journal of Machine Tools & Manufacture*, 47, 2133-2139.
- Lin, Q.Q., Zhang, X.B., Wang, Z.Q., 2010. Study on bottom compression-drawing of boss deforming on plate. *Forging & Stamping Technology*, 35(6), 53-57. (in Chinese)
- Mori, K., Abe, Y., Osakada, K., Hiramatsu, S., 2011. Plate forging of tailored blanks having local thickening for deep drawing of square cups. *Journal of Materials Processing Technology*, 211(10), 1569-1574.
- Merklein, M., Koch, J., Opel, S., Schneider, T., 2011. Fundamental investigations on the material flow at combined sheet and bulk metal forming processes, *CIRP Annals-Manufacturing Technology*, 60(1), 283-286.
- Merklein, M., Allwood, J.M., Behrens, B.-A., Brosius, A., Hagenah, H., Kuzman, K., Mori, K., Tekkaya, A.E., Weckenmann, A., 2012. Bulk forming of sheet metal, *CIRP Annals-Manufacturing Technology*, 61(2), 725-745.
- Sheng, Z.Q., Shivpuri, R., 2006. A hybrid process for forming thin-walled magnesium parts. *Materials Science and Engineering: A*, 428(1-2), 180-187.
- Schneider, T., Merklein, M., 2011. sheet-bulk metal forming of preformed sheet metal parts. *Key Engineering Materials*, 473, 83-90.
- Wang, Z.G., Morishita, K., Ando, T., 2012. Boss forming technology by bottom compression drawing. *Journal of the JSPS*, 53(616), 429-433. (in Japanese).
- Wang, Z.G., Karasawa, M., Katoh, W., 2012. Boss forming limit by bottom compression drawing. *Journal of the JSPS*, 53(616), 434-438. (in Japanese).
- Wang, Z.G., Yoshikawa, Y., Osakada, K., 2013. A new forming method of solid bosses on a cup made by deep drawing. *CIRP Annals-Manufacturing Technology*, 62, 291-294.